TISSUE ENGINEERING: Part A
Volume 19, Number S1, 2014

DOI: 10.1089/ten.tea.2013.0416

YIC Special Issue

Behavior of Encapsulated MG-63 Cells in RGD and Gelatine-Modified Alginate Hydrogels

Alexandra Grigore, MSc,[1,2,*] Bapi Sarker, MSc,[1] Ben Fabry, Dr.-Ing,[2] Aldo R. Boccaccini, Dr.-Ing,[1] and Rainer Detsch, Dr.-Ing[1]

Achieving cell spreading and proliferation inside hydrogels that are compatible with microencapsulation technology represents a major challenge for tissue engineering scaffolding and for the development of three-dimensional cell culture models. In this study, microcapsules of 650–900 μm in diameter were fabricated from oxidized alginate covalently cross-linked with gelatine (AlGel). Schiff's base bond formed in AlGel, detected by Fourier transform infrared spectroscopy, which confirmed the cross-linking of oxidized alginate with gelatine. Biological properties of alginate based hydrogels were studied by comparing the viability and morphology of MG-63 osteosarcoma cells encapsulated in gelatine and RGD-modified alginate. We hypothesized that the presence of gelatine and RGD will support cell adhesion and spreading inside the microcapsules and finally, also vascular endothelial growth factor (VEGF) secretion. After 4 days of incubation, cells formed extensive cortical protrusions and after 2 weeks they proliferated, migrated, and formed cellular networks through the AlGel material. In contrast, cells encapsulated in pure alginate and in RGD-modified alginate formed spherical aggregates with limited cell mobility and VEGF secretion. Metabolic activity was doubled after 5 days of incubation, making AlGel a promising material for cell encapsulation.

Introduction

Effective cell encapsulation relies on the suitable immobilization of cells within a semipermeable biocompatible material. Hydrogels are the materials of choice for cell encapsulation strategies,[1] because they protect the enclosed cells from mechanical stress and they are easy to implant, for example by an injection.[2] Permitting the bidirectional diffusion of nutrients, oxygen, and waste, cells can be kept alive for a long time period in hydrogel matrices.[3,4] There is an increasing need for three-dimensional (3D) culture models in many biomedical areas such as tissue engineering, cell therapy, drug/toxicity screening, and tumour growth modeling.[5] Cells alter their metabolism and functionality in standard two-dimensional cell culture systems due to their inability to form contacts with other cells and with their microenvironments.[6] A system that can mimic the structural architecture and biological functions of the extracellular matrix (ECM) in 3D should satisfy the following characteristics: have suitable mechanical properties and chemical composition, support cell growth and maintenance, and facilitate nutrient, gas, metabolic waste transport, and signal transduction.[7,8] Beyond these basic requirements, the matrix should also be able to support angiogenesis for an effective regeneration purpose in case of vascularized tissues, such as the bone.[9,10] Therefore, encapsulated cells should express vascular endothelial growth factor (VEGF), the major angiogenic factor involved in physiological and pathological angiogenesis.[11]

Given that hydrogels are the most promising materials for 3D cell cultures due to their ability to recreate an aqueous microenvironment, they are often used in conjunction with cell microencapsulation technology.[12–14] Alginate, a well-known natural biopolymer, is a biocompatible polysaccharide extracted from brown algae that forms a stable hydrogel by cross-linking with calcium ions.[15] Its biocompatibility, mild gelling behavior at room temperature, and tunable properties make alginate the most suitable material for cell encapsulation.[1] However, alginate is an inert material and does not promote cell attachment in its pure state.[16] Other potential disadvantages include a slow degradation rate by release of calcium ions and high viscosity at relatively low concentrations, leading to large shear forces that are detrimental to the encapsulated cells. Since cell adhesion and migration are critical conditions for high cell viability and proliferation, modification of the alginate matrix using cell-adhesive ligands (peptides or proteins) has been proposed.[17] For example, alginate has been covalently modified with RGD peptide sequence (Arg-Gly-Asp) by binding to the carboxylic acid functional group through carbodiimide

[1]Institute of Biomaterials, University of Erlangen-Nuremberg, Erlangen, Germany.
[2]Biophysics Group, University of Erlangen-Nuremberg, Erlangen, Germany.
*Current affiliation: Institute of Biotechnology, Department of Chemical Engineering and Biotechnology, University of Cambridge, United Kingdom.

chemistry.[1,18] In addition, an enzymatically cleavable peptide has been incorporated in alginate that supported cell spreading in 3D.[19] Moreover, different proteins and other natural polymers have been added to alginate such as fibrin,[20] collagen,[21] chitosan,[22] and hyaluronic acid.[23] Gelatine is a protein that is obtained by thermal denaturation of collagen from animal skin and bones. Gelatine is used in biomedical applications due to its biocompatibility, cell adhesiveness, enzymatic degradation,[24] decreased immunogenicity, and cost effectiveness.[25] However, in its native state, gelatine has poor mechanical properties and it is water soluble at body temperature. In order to be used as cell-anchorage support, gelatine is usually cross-linked with toxic chemical agents such as glutaraldehyde, acyl azides, and diisocyanates. Gelatine has been added to different polysaccharides such as chitosan[26] and alginate,[27,28] and it has been chemically cross-linked. This step makes gelatine unsuitable for cell encapsulation, which requires mild gelling conditions in the presence of cells. Previous studies investigated a method for directly cross-linking alginate chains with gelatine molecules.[29–32] The covalent bonding occurs through the formation of Schiff's bases between the amino groups of lysine and hydroxylysine groups of gelatine and the aldehyde groups of oxidized alginate. High concentrations (15–20 w/v%) of alginate and gelatine have been used for *in situ* forming hydrogels for wound-dressing applications or bone tissue engineering.[33,34]

The aim of this work was to investigate cross-linked alginate-gelatine (AlGel) microcapsules intended for cell encapsulation and to compare the cell behavior of MG-63 osteoblast-like cells in this novel matrix with that in pure alginate. In addition, a commercially available RGD-modified alginate was investigated in comparison with AlGel. One area of interest for the development of a functional hydrogel that supports cell attachment and spreading as well as high VEFG-release in tissue engineering. Alternative proposed applications include cell delivery and 3D models for cell culture and drug screening.

Materials and Methods

Materials synthesis

Three matrices were investigated in this study: alginate, RGD-modified alginate (RGD-Alginate), and alginate-gelatine cross-linked (AlGel). Alginate (sodium salt of alginic acid from brown algae, suitable for immobilization of micro-organisms, MW 100,000–200,000 g/mol, guluronic acid content 65–70%; Sigma-Aldrich) was dissolved in phosphate buffer saline (PBS; Gibco) and obtained final concentrations of 1.5% (w/v). Gelatine (Type A, porcine skin; Sigma-Aldrich) was dissolved in deionized water (Millipore) at 40°C and obtained a final concentration of 5% (w/v). The solutions were sterilized by sterile filtration with 0.22 μm filters (Roth). RGD-Alginate was obtained by mixing RGD-alginate (Novatech G RGD; Novamatrix) with alginate (Sigma-Aldrich) to obtain a final concentration of 100 μM RGD, which showed the highest cell adhesion of MG-63 in preliminary tests (data not shown). The final alginate concentration of RGD-alginate solution was kept at 1.5% (w/v). Oxidation of alginate was performed in an equal volume of ethanol-water mixture to facilitate cross-linking the polysaccharide, alginate with the protein, gelatin.[35–38] Briefly, 5 g of alginate were dispersed in 25 mL ethanol (VWR) and mixed with 25 mL aqueous solution of sodium metaperiodate (7.5 mmol). The resulting solution was continuously stirred in dark condition at room temperature. The reaction was quenched after 6 h by adding 5 mL of ethylene glycol under continuous stirring for 30 min. The resultant solution was dialyzed against deionized water using a dialysis membrane (MWCO: 6000–8000; Spectrum Lab) for 7 days with several changes of water until the dialysate was periodate free. The absence of periodate was checked by adding a 0.5 mL aliquot of the dialysate to 0.5 mL of a 1% solution of silver nitrate and ensuring the absence of any precipitate. The dialyzed alginate dialdehyde (ADA) solution was frozen and lyophilized. Aqueous solution of gelatine was added slowly in the solution of ADA (in PBS) under continuous stirring to facilitate the cross-linking of ADA with gelatine.[39] The final concentrations of both ADA and gelatine were 2.5% (w/v) in the cross-linked hydrogel. The diameter of the capsules fabricated from three different materials was determined by analyzing 30 capsules of each material using light microscopy (LM, Primo Vert; Carl Zeiss). Chemical characterization was also carried out using Fourier transform infrared spectroscopy (FTIR) to determine the interactions (chemical bonding structure) between the alginate and gelatine components in the fabricated capsules. Films of alginate, gelatine, and AlGel were made by casting the corresponding hydrogels into a polystyrene Petri dish, allowing it to dry for 3 days at room temperature. The dried films were used to record ATR-FTIR spectra using an FTIR spectrometer (Nicolet 6700; Thermo Electron).

The degradation behavior of the hydrogels was determined by measuring the mechanical properties during an incubation period of 28 days. Sterile cylindrical films with a diameter of 16 mm and a thickness of about 1 mm were produced. To mimic cell culture conditions over the whole incubation time, the films were stored in a 24-well plate in a humidified atmosphere with 5% CO_2 at 37°C, covered with 1 mL Dulbecco's modified Eagle's medium (DMEM). By the use of a dynamic mechanical thermal analyzer (DMTA; Rheometric Scientific), the samples were subjected to deformation by compression. The measurements were performed at 25°C in a dynamic frequency sweep, at which a sinusoidal deformation of constant amplitude (0.1 to 25 Hz) was applied on the samples. All measurements were carried out in the linear viscoelastic regime with a strain of 0.1%. The storage modulus (E′) and tangent delta (tan δ) were documented. The storage modulus represents the non-dissipative component of the mechanical properties of a viscoelastic material. The phase angle (δ) is defined by $\tan^{-1}$ (E″/E′), where E″ is the loss modulus. The phase angle indicates whether a material is solid with perfect elasticity ($\delta = 0°$), liquid with pure viscosity ($\delta = 90°$), or exhibits intermediate behavior ($0° < \delta < 90°$). Each measurement was performed thrice on at least two different disk specimens from the same hydrogel sample.

Cell culture and cell encapsulation

Cell cultivation. MG-63 osteoblast-like cells (Sigma-Aldrich) were cultured at 37°C in a humidified atmosphere of 95% air and 5% CO_2, in DMEM (Gibco) supplemented with 10 vol.% fetal bovine serum (FBS; Sigma-Aldrich) and

1 vol.% penicillin/streptomycin (PS; Sigma-Aldrich). Cells were grown for 48 h to confluence in 75 cm^2 culture flasks (Greiner-Bio One), washed with PBS, detached using Trypsin/EDTA (Sigma), and counted by a hemocytometer (Roth). Cell concentration was established by diluting with culture medium.

Cell encapsulation. For cell encapsulation, a cell concentration of 10^6 cells/mL of hydrogel was used. The volume of cell suspension with regard to the total volume of hydrogel solution was kept at 1%, to prevent any change in material concentration and viscosity. The cell suspension was centrifuged for 5 min at 1200 rpm (Centrifuge 5810R; Eppendorf) and re-suspended in culture medium, depending on the amount of cells needed. The cell-polymer mixture was transferred to an extrusion cartridge (Nordson EFD) and connected to a high-precision fluid dispenser (Ultimus V; Nordson EFD). The mixture was extruded by applying different pressures ranging from 0.4 to 2 bars, depending on the material. The capsules were collected in a beaker containing sterile 0.1 M calcium chloride solution. After cross-linking for 10 min, the capsules were sieved using cell culture inserts (Cellcrown; Scaffdex) with a nylon mesh (100 µm pore size; Amazon) as bottom. Capsules were washed thrice with DMEM and cultured in six-well plates in DMEM supplemented with 10 vol.% FBS and 1 vol.% PS. Well plates were incubated with shaking at 150 rpm (MS1 Minishaker; IKA) for a better nutrient diffusion.

Cell viability measurement. Metabolic activity was measured through the reduction of resazurin (Alamar Blue assay; Invitrogen) to resorufin inside the viable cells. A solution of 10% Alamar Blue in medium was added in each well, and the plates were incubated for 3–4 h. After a visible change in color from blue to pink, the absorbance at 570 and 600 nm was measured with a spectrophotometer (Specord 40; Analytik Jena). Live/dead staining of the cells was performed using calcein (Fluka Analytical) for the live cells and propidium iodide (PI; Sigma-Aldrich) for the dead cells. Additional nuclear staining with Höchst (Sigma-Aldrich) was done to improve cell visualization and counting. Staining was performed in 35 mm culture dishes (Greiner) containing capsules. The staining mixture was prepared by mixing 2 mL medium with 2 µL calcein (10 mg/mL), 2.5 µL Höchst and 3 µL PI (1 mg/mL). After replacing the culture medium with staining mixture, the capsules were incubated for 30–60 min and imaged using a fluorescence microscope (FM, DMI 6000B; Leica).

To quantify cell viability, the mitochondrial activity of MG63 cells in different hydrogels was assessed through the enzymatic conversion of tetrazolium salt (WST-8 assay kit; Sigma Aldrich) after 48 h, 5, 7, 10, 14, and 21 days of cultivation. The culture medium was completely removed from the incubated capsules and subsequently added 1% (v/v) to WST-8 assay kit containing culture medium, which was incubated for 2 h. One hundred microliters of supernatant from each sample was transferred into a well of a 96-well plate, and the absorbance at 450 nm was measured with a microplate reader (PHOmo, autobio labtec instruments co. Ltd.).

VEGF release. VEGF secretion from the encapsulated cells was measured by performing a quantitative enzyme-linked immunosorbent assay (Human VEGF ELISA Kit; RayBio®). After 48 h of cultivation, 100 µL supernatant of each sample were collected and prepared according to the manufacturer's instructions. The optical density of each well was determined using a microplate reader at a 450 nm test wavelength. The VEGF-release from MG-63 cells in the different capsules was calculated by a standard curve.

Cell morphology. Cell morphology and cell distribution in 3D were assessed by FM (DMI 6000B; Leica). Live cells were stained with calcein and Höchst (2 µL calcein, 2.5 µL Höchst per 35 mm culture dish) and incubated for 20–30 min. Actin cytoskeleton staining was performed using the following protocol: Samples were washed twice with Hank's balanced salt solution (HBSS; SAFC Biosciences), followed by room temperature fixation for 20 min in 4% paraformaldehyde (Thermo Scientific) solution in HBSS. Afterward, samples were washed thrice with HBSS, and membrane permeabilization was done for 5 min using 0.1% Triton-X 100 (Sigma-Aldrich) in HBSS. After washing thrice with HBSS, samples were incubated for 1 h at 37°C with 0.5% bovine serum albumin (BSA; Sigma-Aldrich) in HBSS to avoid nonspecific binding. Phalloidin (Sigma-Aldrich) in 1:1000 dilution in HBSS was added and incubated for 1 h at 37°C. Samples were finally washed thrice and stored in HBSS with 0.5% BSA. Cell morphology was analyzed by confocal laser scanning microscopy (CLSM, DM6000 CFS; Leica). Capsules were prepared for scanning electron microscopy (SEM) imaging by fixation and dehydration with an ethanol series from 30% to 99.8% ethanol concentration. Each dehydration step was set to 1 h in order to insure complete diffusion of ethanol inside the capsule. Samples were subsequently dried using a critical-point drying device (EMCPD 300; Leica). Capsules were glued on the sample holder using a double-adhesive sticker and imaged with SEM at a voltage of 1 kV (ULTRA 55 FE SEM; Carl Zeiss).

Statistical analysis

Results for cell viability ($n = 4$–8 samples) and live/dead counting ($n = 10$ capsules) are presented as arithmetic mean

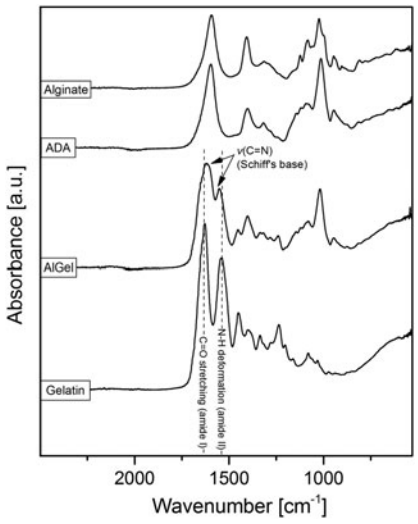

FIG. 1. ATR-FTIR spectra of alginate, ADA, AlGel, and gelatine. FTIR, Fourier transform infrared spectroscopy; ADA, alginate dialdehyde; AlGel, alginate-gelatine.

and standard deviations. Differences between materials tested were evaluated by one-way analysis of variance. The level of statistical significance was established at $p < 0.05$ or $p < 0.01$ (Origin 8.5G; OriginLab Corporations).

Results and Discussion

FTIR spectra of alginate, ADA, and AlGel shown in Figure 1, exhibited the peaks at 1000–1125 and 1240 cm^{-1} regions, which confirmed the presence of guluronic acid, mannuronic acid, and o-acetyl ester, the building blocks of alginic acid. The peaks at 1621 and 1557 cm^{-1} correspond to Schiff's base bond, which confirmed the cross-linking of alginate and gelatin.[40] Moreover, the peak at 1621 cm^{-1} due to Schiff's base bond overlapped with the band at 1630 cm^{-1} of amide I of uncrosslinked gelatin, which made the corresponding peak broader in AlGel compared with alginate and ADA.[39,41]

Figure 2 shows the results of DMTA measurements of alginate and AlGel material at different points over a frequency range from 0.1 to 15 Hz in a double logarithmic plot. Immediately after their preparation (day 0), all materials showed typical viscoelastic behavior, namely showing an increase of the storage modulus with frequency. Furthermore, all materials exhibited storage moduli values in the same order of magnitude, ranging from around 400 kPa at 0.1 Hz to around 600 kPa at 15 Hz. After 3 days of incubation, the storage modulus started decreasing, especially for AlGel material. With increasing incubation time, the storage moduli of all materials decreased, which is a result of the material's degradation. In all hydrogels, gelation of alginate takes place by the formation of egg boxes in the presence of Ca^{2+}. This gelling reaction can be reversed by removing these divalent cations.[42] Since this process occurs with time because of a diffusion mechanism, the hydrogel network is destabilized and the alginate polymer chains get solubilized. Therefore, the materials become softer. Another reason for this behavior is that hydrogels tend to imbibe water due to osmotic forces. It is likely that the periodate oxidation reaction which turns alginate to ADA specifically cleaves vicinal glycols mostly in the G-units of the alginate polymer.[39,43] As a result, the ionic gelation property of ADA is reduced due to the lack of available G-units. Since these oxidized residues are not bound firmly to the gel network, these are probably more accessible toward degradation than unoxidized residues.[44] Since more reactive hydroxyl groups are present in ADA, hydrolysis is improved compared with unmodified alginate.[35] In addition to that, the oxidized residues are very susceptible to alkaline β-elimination, which further enhances the degradability of ADA in physiological conditions.[44] Consequently, samples made of AlGel material show a higher level of degradation after 28 days of incubation as compared to pure alginate. After 28 days of incubation, the storage moduli of alginate and AlGel hydrogels are 196 and 113 kPa, respectively, at the frequency of 15 Hz. All materials exhibited viscoelastic behavior, as the loss factor (tan δ) is always between 0 and 1. With increasing incubation time, the viscous properties of all materials increased. The degradation behavior of the materials is responsible for the softening of the hydrogels, leading to an increase of viscous properties.

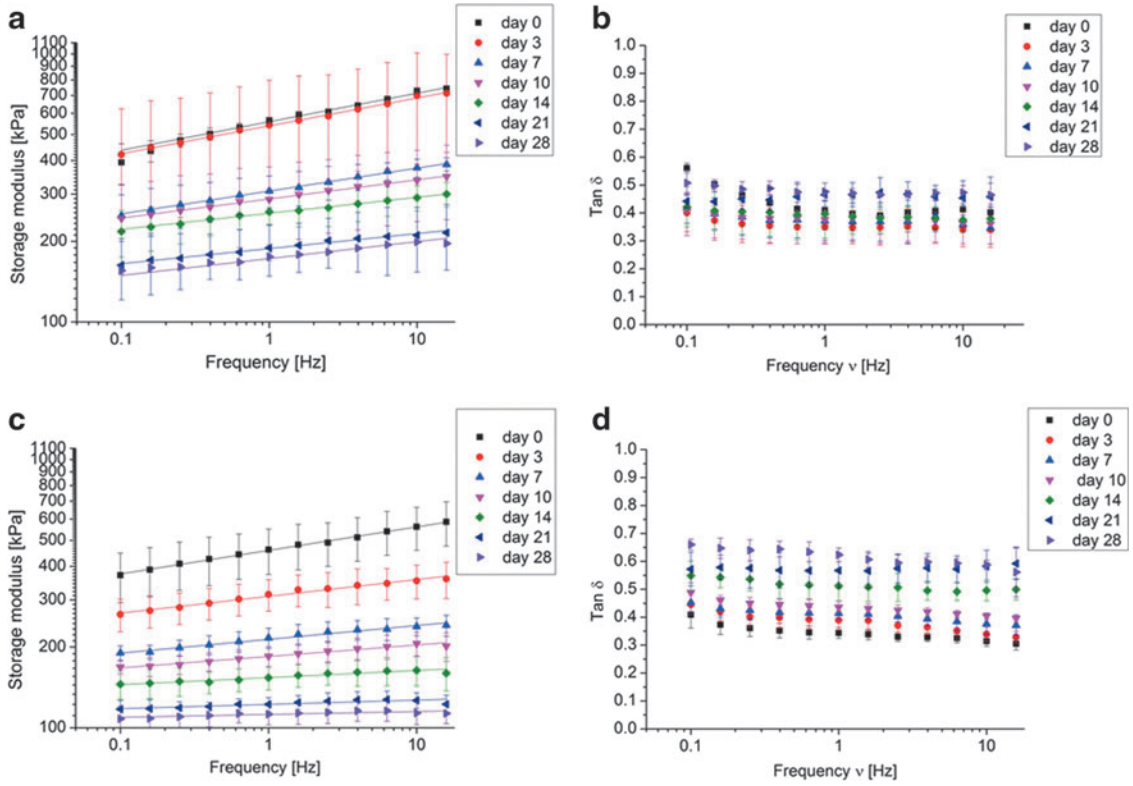

FIG. 2. Storage modulus of alginate **(a)** and AlGel **(c)** over a frequency range from 0.1 to 15 Hz at T = 25°C (right). Tan delta of alginate **(b)** and AlGel **(d)** at different points of time over a frequency range from 0.1 to 15 Hz (T = 25°C).

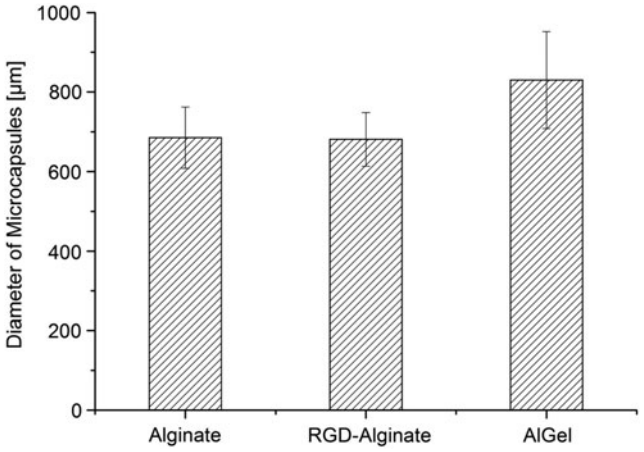

FIG. 3. Diameter of fabricated capsules from alginate, RGD-alginate, and AlGel hydrogels.

Consequently, the AlGel material shows the highest values of loss factor during the incubation period due to its high degradation behavior.

With regard to the hydrogel degradation and its influence on the mechanical properties of the materials, it should be considered that in DMTA, stress is applied on the hydrogels, which can influence gel composition and mechanical stability. All DMTA measurements were carried out over a frequency range of 0.1 to 16 Hz, which covers the characteristic timescales of periodic loads, which also occur in the body.[45]

In this study, microcapsules of AlGel of sizes ranging from 650 to 900 µm (Fig. 3) were fabricated by the innovative method presented earlier. The morphology of AlGel is very different from that of alginate or RGD-alginate.

Figure 4a–c shows light microscope images of MG-63 cells encapsulated in different materials after fabrication. Alginate (Fig. 3a) and RGD-Alginate (Fig. 3b) capsules have a spherical shape and smooth surface, whereas AlGel (Fig. 3c) capsules are distorted spheres with a rough surface and inhomogeneous composition. It was measured that the capsules fabricated from AlGel are slightly larger than those of alginate and RGD-alginate (see Fig. 3). This result can be explained by the less ionic gelation properties of AlGel hydrogel compared with alginate and RGD-alginate, given that the chemical cross-linking process during synthesis of AlGel could hamper the ionic gelation character of alginate. Moreover ADA synthesized from alginate possesses a comparatively lower-molecular weight and viscosity than alginate that could also hamper its ionic gelation character.

SEM images (Fig. 5) show typical microcapsule surfaces of different materials after 2 days of incubation. During this cultivation period, no cells on the outer surface could be detected. It was observed that ionically cross-linked alginates are nano-porous and form regular patterns in the form of folds or wrinkles. The microcapsule surfaces were seen to become less folded in RGD-Alginate in comparison to pure alginate corresponding to a decrease in molecular weight. However, AlGel capsules were observed to have a highly inhomogeneous surface without any regular pattern. A crack in the material surface reveals the internal structure of AlGel, showing a highly porous matrix with channels of ~5–30 µm (Fig. 5f).

Innovative soft materials that support cell attachment, spreading, and proliferation are needed for cell encapsulation in novel applications in regenerative medicine. While alginate has been proved to be a suitable material for microencapsulation, it does not possess cell-adhesion cues and often does not support cell proliferation. Modification of alginate with different molecules such as RGD peptide or fibrin leads to an increased cell viability, but cell morphology remains mainly spherical. A good cell spreading inside alginate hydrogels has been obtained only after double modification with RGD and an enzymatically cleavable peptide.[19] Cell proliferation inside alginate hydrogel is controversially presented in the literature: Some studies show no proliferation, while others report that alginate supports cell proliferation.[46–51] It is, therefore, desirable to find a method for alginate modification that is fast, cost effective, and promotes cell spreading and proliferation while also being compatible with microencapsulation technology. In this study, alginate cross-linked with gelatine was synthesized and investigated as a potential material for cell encapsulation. The main goal was to improve the biological properties of nonmodified or oxidized alginate to achieve superior performance as compared with existing commercial RGD modified alginate. By incorporating gelatine into oxidized alginate, we address at least two of the major challenges for creating suitable 3D matrices: incorporation of cell-adhesion ligands to enable cell-matrix interaction and degradation sites to enable matrix remodeling.

Typical fluorescent images of live/dead stained MG-63 cells in both alginate and AlGel after 2 days of incubation are shown in Figures 6a and 6b. The small amount of dead cells (red) compared with live cells (green) confirms that none of the materials exhibits cytotoxicity. The fabrication of the capsules using the pneumatic pressure of 0.4 to 2 bars

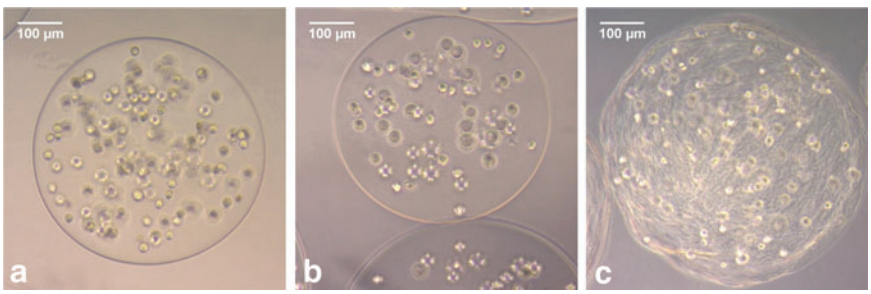

FIG. 4. LM images of MG-63 cells encapsulated in different materials after fabrication: Alginate **(a)**, RGD-Alginate **(b),** and AlGel **(c)**. LM, light microscopy.

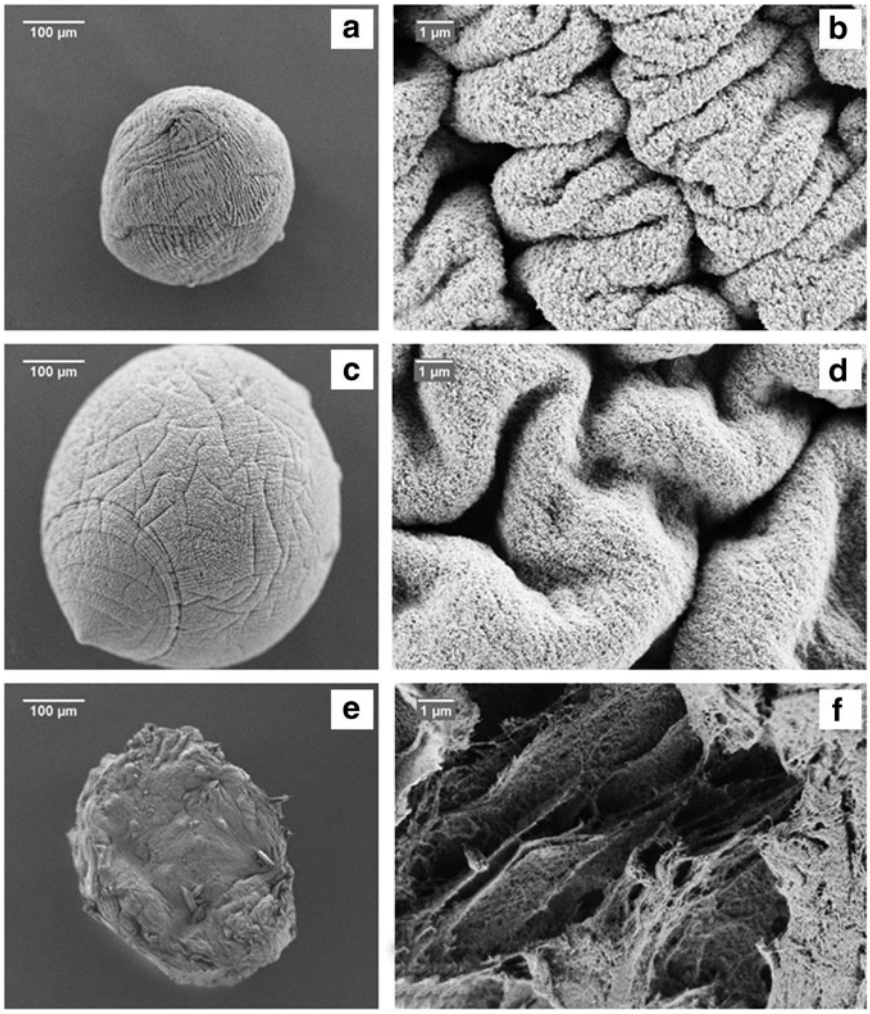

FIG. 5. Scanning electron microscopy images at different magnifications of dehydrated and dried capsules of different materials after 2 days of cultivation: alginate **(a, b)**, RGD-Alginate **(c, d)**, and AlGel **(e, f)**.

also seems to have no influence on the viability of MG-63 cells. Quantitative assessment of the cell viability during 21 days of cultivation is shown in Figure 6c. The increase of cell viability is similar in all matrices during the first week of incubation; whereas afterward, there is a substantial difference in the measured cell viability. Cells immobilized in AlGel exhibit a significantly higher mitochondrial activity compared with alginate and RGD-Alginate after 10–21 days of cultivation.

In Figure 7, the VEGF release from MG-63 cells encapsulated in alginate, RGD-Alginate and AlGel after 48 h of cultivation is shown. Compared with the present study, immobilized fibroblasts in 2 wt% alginate capsules showed continued expression and release of VEGF over 21 days of cultivation.[52] While the immobilized osteoblast-like cells secrete a similar amount of VEGF from alginate and RGD-Alginate, significantly enhanced VEGF secretion from AlGel was measured in the cell culture medium. Numerous studies have demonstrated the critical role of angiogenesis in successful tissue integration during bone fracture repair.[11] VEGF is well known as an effective endothelial cell-specific stimulus. Thus, the release of VEGF from immobilized cells in soft matrices should correlate with the observed increase in the angiogenic potential of such matrices. Therefore, the amount of expressed VEGF in cells immobilized in a hydrogel could depend on the chemical composition of the matrix as well as on the microenvironmental conditions, for example, the level of oxygen. The VEGF release could further depend on the presence and concentration of collagenases, enzymes that are considered to be released from invading cells, for example, fibroblasts and lymphocytes. Moreover, to enhance the VEGF secretion of cells in alginate, colloidal suspensions of bioactive glass (BG) particles could be added in specific concentrations given the effect of dissolution products of BG on VEGF secretion.[53] For example, Keshaw *et al.* showed that a concentration of 0.1% (w/v) of BG induced a significantly higher VEGF expression than lower and higher concentrations. Furthermore, other studies have shown that RGD-modified alginate improved the angiogenic potential through differentiation of human mesenchymal stem cell into the osteogenic lineage.[53]

In Figure 8, the metabolic activity of MG-63 cells encapsulated in alginate, RGD-Alginate, and AlGel is shown after 2 and 5 days of incubation. The metabolic activity of cells in AlGel doubles after 5 days of incubation, as compared with alginate and RGD-Alginate. High metabolic activities of MG-63 osteoblast-like cells prove that AlGel presents no cytotoxity: 93% of the cells in AlGel were alive, suggesting that the number of aldehyde groups was reduced

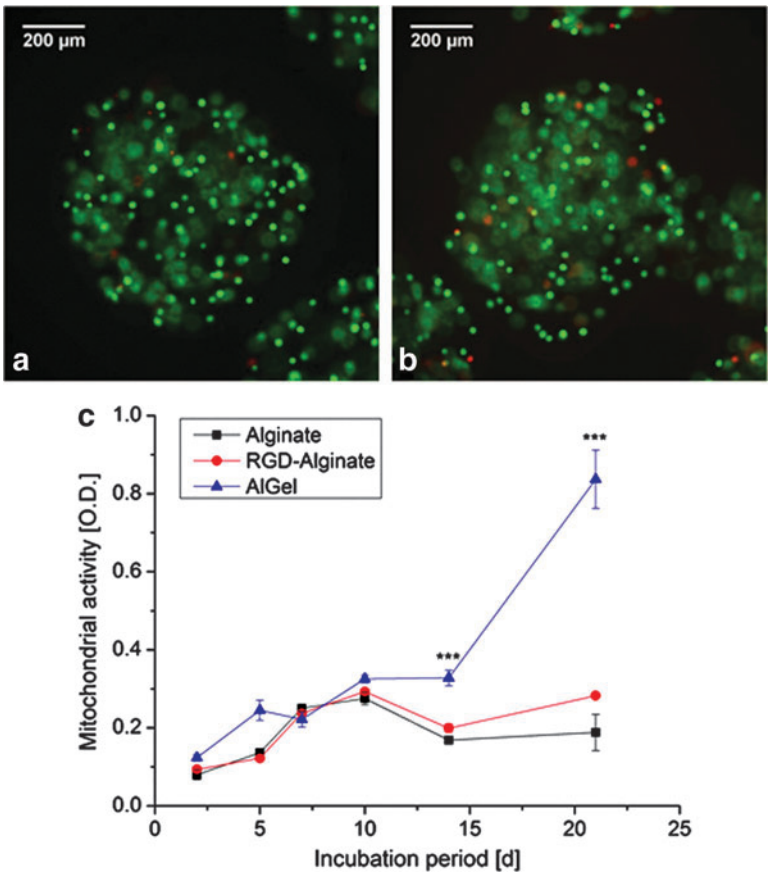

FIG. 6. Fluorescence microscopy images of MG-63 cells incubated for 2 days in alginate **(a)** and AlGel **(b)**; Green: calcein-stained live cells; Red: propidium iodide-stained dead cells. **(c)** Mitochondrial activity of MG-63 cells immobilized in alginate, RGD-Alginate, and AlGel over the different time of incubation. ***$p < 0.001$ compared with alginate.

by gelatine cross-linking. Metabolic activity results after 2 and 5 days are in accordance with the live/dead assay: alginate and RGD-Alginate showed no significant differences. However, cells in AlGel exhibited an increased metabolic activity of 125% as compared with alginate after 2 days of incubation. Furthermore, the observed VEGF release profile (Fig. 7) can be explained by the high cell metabolic activity and by the strong attachment of the cells to the matrices.

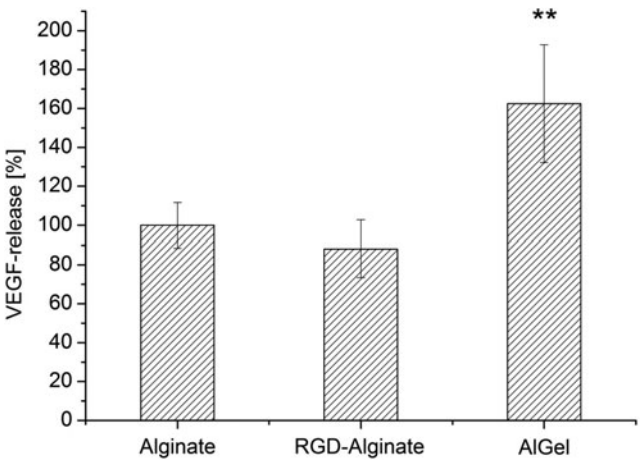

FIG. 7. Vascular endothelial growth factor release from MG-63 cells immobilized in alginate, RGD alginate, and AlGel after 48 h of incubation. **$p < 0.01$ compared with alginate.

This behavior can be explained by the formation of cell-matrix contacts in the cross-linked material, leading to more viable cells. In contrast, metabolic activity of MG-63 cells in AlGel drastically increased after 5 days to almost 200%. A reason for this behavior is likely related to the differences in morphology between cells encapsulated in alginate, RGD-Alginate and AlGel hydrogels.

CLSM images of MG-63 cells encapsulated in alginate, RGD-Alginate, and AlGel incubated for 4 days are shown in Figure 9a–c. The typical morphology of cells entrapped in alginate is spherical and even after proliferation, cell clusters are seen to be spherical (Fig. 9a). RGD-Alginate promotes the formation of small actin protrusions in the surrounding matrix, but the cells maintain their spherical shape (Fig. 9b). After 14 days (Fig. 9d–f), cell clusters remain spherical in alginate; whereas cells migrate and spread through AlGel forming cell chains through the entire microcapsule (Supplementary Figs. S1–S3; Supplementary Data are available online at www.liebertpub.com/tea). Cells encapsulated in AlGel display multiple elongated protrusions and even formation of cell–cell contacts over distances larger than 30 µm (Supplementary Fig. S1a). Cells encapsulated in alginate for approximately 6 weeks form compact aggregates that grow in sizes ranging from 30 to 300 µm in diameter (Supplementary Fig. S2). No cell-material contact or cell migration out of the clusters can be observed. In contrast, cells cultured in AlGel form randomly shaped clusters or cell chains (Supplementary Fig. S2b). The typical cell morphology inside alginate hydrogels is spherical, as imaged by FM and no cell-matrix interactions could be

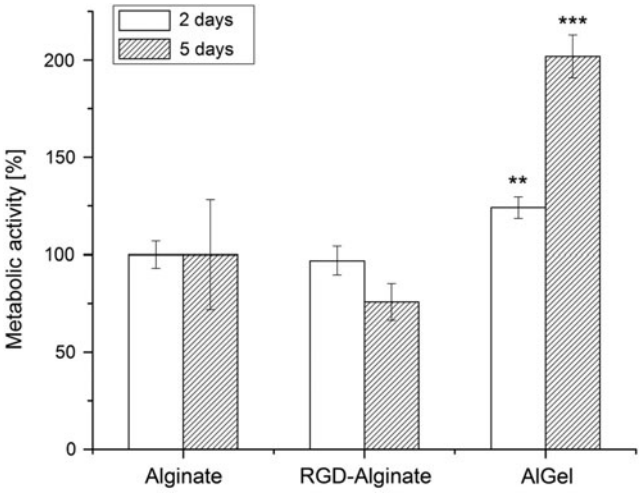

FIG. 8. Metabolic activity of MG-63 cells after 2 and 5 days of incubation, encapsulated in alginate, RGD-modified alginate, and alginate cross-linked with gelatine (AlGel). $^{**}p < 0.01$ and $^{***}p < 0.001$ compared with alginate.

noticed.[54] Formation of spherical aggregates has been observed in the literature for hematopoetic stem cells and human embryonic stem cells.[55,56] Cells encapsulated in RGD-Alginate maintained the same round-shape morphology, but, in addition, presented a few cortical protrusions through the surrounding matrix, with their size not exceeding 2–3 μm (Fig. 9b). Similar observations of cells encapsulated in RGD-Alginate have been reported in literature.[57] A different behavior is observed for the cells embedded in AlGel, where cells formed multiple actin protrusions through the matrix and often formed cell–cell contact over large distances. These findings are in accordance to the viability data, showing that both cell–material and cell–cell contacts lead to increased metabolic activity. After 2 weeks of incubation, cells encapsulated in AlGel presented elongated morphologies and migrated, forming cell chains throughout the material (Fig. 9f and Supplementary Figs. S1 and S2).

The cell proliferation ability inside alginate capsules is controversially discussed in the literature. While hepatocytes clearly proliferate and form cell spheroids and endothelial cells are able to proliferate and migrate through the gel, their behavior is not so clear for other types of cells.[58] For example, in one study, osteoblast-like cell (MC3T3-E1) number was seen to decrease over the course of 30 days when immobilized in alginate and RGD-Alginate; while another study states that the same type of cells proliferate in RGD-Alginate.[59] Fibroblasts proliferate inside RGD-Alginate and cardiomyocites proliferate and form organized layers.[50] In the present study, after 3 weeks of incubation, cells cultured inside AlGel migrated and proliferated through the material, demonstrating an effective cell–matrix interaction. This behavior is a direct consequence of material properties such as stiffness and pore size distribution. It has been shown in literature that oxidized alginate cross-linked with gelatine at high concentrations (15–20%) forms a porous hydrogel which supports cell proliferation.[31,38,59] It can be assumed that a similarly porous material is formed at low concentrations (e.g., 2% used in this study). This assumption was validated by SEM morphological analysis, where long pores of several microns could be visualized inside the AlGel capsules (Fig. 4c). Moreover, literature studies show that a fast degradation of the cross-linked material occurs in the first 2 weeks and a complete dissolution takes place after 5 weeks.[7,29] Even if in these studies no additional cross-linking with calcium ions was performed, it can be assumed that the degradation of the AlGel material is faster than that of pure alginate, explaining a higher porosity. The most widely investigated method for alginate modification remains RGD incorporation. However, the chemical modification process involves several steps, being relatively expensive and time consuming.

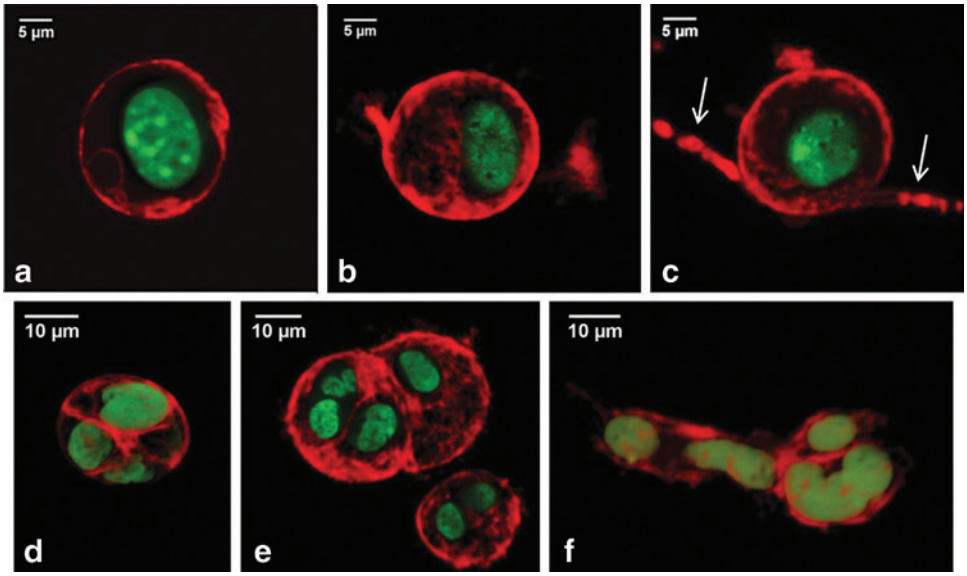

FIG. 9. CLSM images of MG-63 cells (actin cytoskeleton in red and nucleus in green) after 4 days **(a–c)** and 14 days **(d–f)** of incubation, encapsulated in different materials: alginate **(a, d)**, RGD-Alginate **(b, e),** and AlGel **(c, f)**; arrows indicate cortical protrusions. CLSM, confocal laser scanning microscopy.

Conclusions

In order to improve cell behavior, such as increased cell vitality, VEGF secretion, cell anchorage to alginate matrices, and to support cell spreading, the current study has proposed the use of covalently cross-linked alginate and gelatine for cell microencapsulation. Several challenges should be addressed before hydrogel-based tissue constructs can be used in biofabrication approaches for regenerative medicine. In general, the size of the capsules fabricated in this work is too large and, therefore, disadvantageous for the nutrition and the oxygen supply of encapsulated cells. Consequently, current investigations involve the production of uniform capsules with reproducibility in terms of shape and exhibiting smaller size. Furthermore, the ability of other cell types (such as MSCs) to adhere and proliferate in these hydrogels needs to be analyzed. As a result of this work, the physico-mechanical properties of microcapsules should also be determined to understand the *in vitro* degradation mechanism. The mechanical properties of hydrogels itself should be improved by, for example, addition of nanoscale inorganic fillers, that is, creating nanocomposites. In addition, the degradation of cross-linked materials should be adapted to the *in-situ* formation of ECM. Finally, the integration of these materials into biofabrication techniques, for example, cell printing processes, to create hierarchically and intra-complex architectures for tissue mimicking constructs, should be investigated. Thus, further studies of this promising material combination will consider their applicability as a soft matrix for more complex biofabrication approaches.[60]

Acknowledgments

The authors acknowledge support from the ''Emerging Fields Initiative'' of the University of Erlangen-Nuremberg (Germany) (Project: TOPbiomat). Experimental assistance of Huixin Bao and Mathias Hanisch is highly appreciated.

Disclosure Statement

No competing financial interests exist.

References

1. Rowley, J.A., Madlambayan, G., and Mooney, D.J. Alginate hydrogels as synthetic extracellular matrix materials. Biomaterials **20,** 45, 1999.
2. Murua, A., Portero, A., Orive, G., Hernández, R.M., de Castro, M., and Pedraz, J.L. Cell microencapsulation technology: towards clinical application. J Control Release **132,** 76, 2008.
3. Awad, H.A., Wickham, M.Q., Leddy, H.A., Gimble, J.M., and Guilak, F. Chondrogenic differentiation of adipose-derived adult stem cells in agarose, alginate, and gelatin scaffolds. Biomaterials **25,** 3211, 2004.
4. Jen, A.C., Wake, M.C., and Mikos, A.G. Review: hydrogels for cell immobilization. Biotechnol Bioeng **50,** 357, 1996.
5. Lee, J., Cuddihy, M.J., and Kotov, N.A. Three-dimensional cell culture matrices: state of the art. Tissue Eng Part B Rev **14,** 61, 2008.
6. Meli, L., Jordan, E.T., Clark, D.S., Linhardt, R.J., and Dordick, J.S. Influence of a three-dimensional, microarray environment on human Cell culture in drug screening systems. Biomaterials **33,** 9087, 2012.
7. Geckil, H., Xu, F., Zhang, X., Moon, S., and Demirci, U. Engineering hydrogels as extracellular matrix mimics. Nanomedicine **5,** 469, 2010.
8. Tibbitt, M.W., and Anseth, K.S. Hydrogels as extracellular matrix mimics for 3D cell culture. Biotechnol Bioeng **103,** 655, 2009.
9. Mauney, J.R., Volloch, V., and Kaplan, D.L. Role of adult mesenchymal stem cells in bone tissue-engineering applications: current status and future prospects. Tissue Eng **11,** 787, 2005.
10. Kneser, U., Schaefer, D.J., Polykandriotis, E., and Horch, R.E. Tissue engineering of bone: the reconstructive surgeon's point of view. J Cell Mol Med **10,** 7, 2006.
11. Street, J., Bao, M., DeGuzman, L., Bunting, S., Peale, F.V., Jr., Ferrara, N., *et al.* Vascular endothelial growth factor stimulates bone repair by promoting angiogenesis and bone turnover. Proc Natl Acad Sci U S A **99,** 9656, 2002.
12. Slaughter, B.V., Khurshid, S.S., Fisher, O.Z., Khademhosseini, A., and Peppas, N.A. Hydrogels in regenerative medicine. Adv Mater **21,** 3307, 2009.
13. Albrecht, D.R., Underhill, G.H., Wassermann, T.B., Sah, R.L., and Bhatia, S.N. Probing the role of multicellular organization in three-dimensional microenvironments. Nat Methods **3,** 369, 2006.
14. Nicodemus, G.D., and Bryant, S.J. Cell encapsulation in biodegradable hydrogels for tissue engineering applications. Tissue Eng Part B Rev **14,** 149, 2008.
15. Lee, K.Y., and Mooney, D.J. Alginate: properties and biomedical applications. Prog Polym Sci (Oxford) **37,** 106, 2012.
16. Kong, H.J., Smith, M.K., and Mooney, D.J. Designing alginate hydrogels to maintain viability of immobilized cells. Biomaterials **24,** 4023, 2003.
17. Rice, J.J., Martino, M.M., De Laporte, L., Tortelli, F., Briquez, P.S., and Hubbell, J.A. Engineering the regenerative microenvironment with biomaterials. Adv Healthc Mater **2,** 57, 2013.
18. Kang, S.W., Cha, B.H., Park, H., Park, K.S., Lee, K.Y., and Lee, S.H. The Effect of conjugating RGD into 3D alginate hydrogels on adipogenic differentiation of human adipose-derived stromal cells. Macromol Biosci **11,** 673, 2011.
19. Fonseca, K.B., Bidarra, S.J., Oliveira, M.J., Granja, P.L., and Barrias, C.C. Molecularly designed alginate hydrogels susceptible to local proteolysis as three-dimensional cellular microenvironments. Acta Biomater **7,** 1674, 2011.
20. Zhou, H., and Xu, H.H.K. The fast release of stem cells from alginate-fibrin microbeads in injectable scaffolds for bone tissue engineering. Biomaterials **32,** 7503, 2011.
21. Sun, J., Xiao, W., Tang, Y., Li, K., and Fan, H. Biomimetic interpenetrating polymer network hydrogels based on methacrylated alginate and collagen for 3D pre-osteoblast spreading and osteogenic differentiation. Soft Matter **8,** 2398, 2012.
22. Haque, T., Chen, H., Ouyang, W., Martoni, C., Lawuyi, B., Urbanska, A.M., *et al. In vitro* study of alginate-chitosan microcapsules: an alternative to liver cell transplants for the treatment of liver failure. Biotechnol Lett **27,** 317, 2005.
23. Dahlmann, J., Krause, A., Möller, L., Kensah, G., Möwes, M., Diekmann, A., *et al.* Fully defined *in situ* cross-linkable alginate and hyaluronic acid hydrogels for myocardial tissue engineering. Biomaterials **34,** 940, 2013.

24. Gelse, K., Pöschl, E., and Aigner, T. Collagens—structure, function, and biosynthesis. Adv Drug Deliv Rev **55,** 1531, 2003.
25. Tan, H., Chu, C.R., Payne, K.A., and Marra, K.G. Injectable *in situ* forming biodegradable chitosan-hyaluronic acid based hydrogels for cartilage tissue engineering. Biomaterials **30,** 2499, 2009.
26. Huang, Y., Onyeri, S., Siewe, M., Moshfeghian, A., and Madihally, S.V. *In vitro* characterization of chitosan-gelatin scaffolds for tissue engineering. Biomaterials **26,** 7616, 2005.
27. Bernhardt, A., Despang, F., Lode, A., Demmler, A., Hanke, T., and Gelinsky, M. Proliferation and osteogenic differentiation of human bone marrow stromal cells on alginate—gelatine—hydroxyapatite scaffolds with anisotropic pore structure. J Tissue Eng Regen Med **3,** 54, 2009.
28. Almeida, P.F., and Almeida, A.J. Cross-linked alginate-gelatine beads: a new matrix for controlled release of pindolol. J Control Release **97,** 431, 2004.
29. Liao, H., Zhang, H., and Chen, W. Differential physical, rheological, and biological properties of rapid *in situ* gelable hydrogels composed of oxidized alginate and gelatin derived from marine or porcine sources. J Mater Sci Mater Med **20,** 1263, 2009.
30. Balakrishnan, B., and Jayakrishnan, A. Self-cross-linking biopolymers as injectable *in situ* forming biodegradable scaffolds. Biomaterials **26,** 3941, 2005.
31. Balakrishnan, B., Mohanty, M., Umashankar, P.R., and Jayakrishnan, A. Evaluation of an *in situ* forming hydrogel wound dressing based on oxidized alginate and gelatin. Biomaterials **26,** 6335, 2005.
32. Nguyen, T.P., and Lee, B.T. Fabrication of oxidized alginate-gelatin-BCP hydrogels and evaluation of the microstructure, material properties and biocompatibility for bone tissue regeneration. J Biomater Appl **27,** 311, 2012.
33. Augst, A.D., Kong, H.J., and Mooney, D.J. Alginate hydrogels as biomaterials. Macromol Biosci **6,** 623, 2006.
34. Drury, J.L., and Mooney, D.J. Hydrogels for tissue engineering: scaffold design variables and applications. Biomaterials **24,** 4337, 2003.
35. Boanini, E., Rubini, K., Panzavolta, S., and Bigi, A. Chemico-physical characterization of gelatin films modified with oxidized alginate. Acta Biomater **6,** 383, 2010.
36. Manju, S., Muraleedharan, C.V., Rajeev, A., Jayakrishnan, A., and Joseph, R. Evaluation of alginate dialdehyde cross-linked gelatin hydrogel as a biodegradable sealant for polyester vascular graft. J Biomed Mater Res Part B Appl Biomater **98B,** 139, 2011.
37. Sakai, S., Yamaguchi, S., Takei, T., and Kawakami, K. Oxidized alginate-cross-linked alginate/gelatin hydrogel fibers for fabricating tubular constructs with layered smooth muscle cells and endothelial cells in collagen gels. Biomacromolecules **9,** 2036, 2008.
38. Bouhadir, K.H., Lee, K.Y., Alsberg, E., Damm, K.L., Anderson, K.W., and Mooney, D.J. Degradation of partially oxidized alginate and its potential application for tissue engineering. Biotechnol Prog **17,** 945, 2001.
39. Sarkar, B., Papageorgiou, D.G., Silva, R., Zehnder, T., Gul-E-Noor, F., Bertmer, M., *et al.* Fabrication of alginate gelatin crosslinked hydrogel microcapsules and evaluation of the microstructure and physio-chemical properties. J Mater Chem B **2,** 1470, 2014.
40. Ye, J., Xiong, J., and Sun, R. The fluorescence property of Schiff's bases of carboxymethyl cellulose. Carbohydr Polym **88,** 1420, 2012.
41. Issa, R.M., Khedr, A.M., and Rizk, H. 1H NMR, IR and UV/VIS spectroscopic studies of some schiff bases derived from 2-aminobenzothiazole and 2-amino-3-hydroxypyridine. J Chin Chem Soc (Taipei) **55,** 875, 2008.
42. Bajpai, S.K., and Sharma, S. Investigation of swelling/degradation behaviour of alginate beads crosslinked with Ca^{2+} and Ba^{2+} ions. React Funct Polym **59,** 129, 2004.
43. Gomez, C.G., Rinaudo, M., and Villar, M.A. Oxidation of sodium alginate and characterization of the oxidized derivatives. Carbohydr Polym **67,** 296, 2007.
44. Kristiansen, K.A., Tomren, H.B., and Christensen, B.E. Periodate oxidized alginates: depolymerization kinetics. Carbohydr Polym **86,** 1595, 2011.
45. Sobral, J.M., Caridade, S.G., Sousa, R.A., Mano, J.F., and Reis, R.L. Three-dimensional plotted scaffolds with controlled pore size gradients: effect of scaffold geometry on mechanical performance and cell seeding efficiency. Acta Biomater **7,** 1009, 2011.
46. Leal-Egaña, A., Dietrich-Braumann, U., Díaz-Cuenca, A., Nowicki, M., and Bader, A. Determination of pore size distribution at the cell-hydrogel interface. J Nanobiotechnol **9,** 24, 2011.
47. Khattak, S.F., Spatara, M., Roberts, L., and Roberts, S.C. Application of colorimetric assays to assess viability, growth and metabolism of hydrogel-encapsulated cells. Biotechnol Lett **28,** 1361, 2006.
48. Evangelista, M.B., Hsiong, S.X., Fernandes, R., Sampaio, P., Kong, H.J., Barrias, C.C., *et al.* Upregulation of bone cell differentiation through immobilization within a synthetic extracellular matrix. Biomaterials **28,** 3644, 2007.
49. Kong, H.J., Boontheekul, T., and Mooney, D.J. Quantifying the relation between adhesion ligand-receptor bond formation and cell phenotype. Proc Natl Acad Sci U S A **103,** 18534, 2006.
50. Lee, J.W., Park, Y.J., Lee, S.J., Lee, S.K., and Lee, K.Y. The effect of spacer arm length of an adhesion ligand coupled to an alginate gel on the control of fibroblast phenotype. Biomaterials **31,** 5545, 2010.
51. Hunt, N.C., Shelton, R.M., Henderson, D.J., and Grover, L.M. Calcium-alginate hydrogel-encapsulated fibroblasts provide sustained release of vascular endothelial growth factor. Tissue Eng Part A **19,** 905, 2013.
52. Bidarra, S.J., Barrias, C.C., Barbosa, M.A., Soares, R., and Granja, P.L. Immobilization of human mesenchymal stem cells within RGD-grafted alginate microspheres and assessment of their angiogenic potential. Biomacromolecules **11,** 1956, 2010.
53. Keshaw, H., Forbes, A., and Day, R.M. Release of angiogenic growth factors from cells encapsulated in alginate beads with bioactive glass. Biomaterials **26,** 4171, 2005.
54. Hunt, N.C., Smith, A.M., Gbureck, U., Shelton, R.M., and Grover, L.M. Encapsulation of fibroblasts causes accelerated alginate hydrogel degradation. Acta Biomater **6,** 3649, 2010.
55. Yuan, Y., Tse, K.T., Sin, F.W.Y., Xue, B., Fan, H.H., and Xie, Y. *Ex vivo* amplification of human hematopoietic stem and progenitor cells in an alginate three-dimensional culture system. Int J Lab Hematol **33,** 516, 2011.
56. Chayosumrit, M., Tuch, B., and Sidhu, K. Alginate microcapsule for propagation and directed differentiation

of hESCs to definitive endoderm. Biomaterials **31,** 505, 2010.
57. Huebsch, N., Arany, P.R., Mao, A.S., Shvartsman, D., Ali, O.A., Bencherif, S.A., *et al.* Harnessing traction-mediated manipulation of the cell/matrix interface to control stem-cell fate. Nat Mater **9,** 518, 2010.
58. Bidarra, S.J., Barrias, C.C., Fonseca, K.B., Barbosa, M.A., Soares, R.A., and Granja, P.L. Injectable *in situ* cross-linkable RGD-modified alginate matrix for endothelial cells delivery. Biomaterials **32,** 7897, 2011.
59. Cai, K., Zhang, J., Deng, L.H., Yang, L., Hu, Y., Chen, C., *et al.* Physical and biological properties of a novel hydrogel composite based on oxidized alginate, gelatin and tri-calcium phosphate for bone tissue engineering. Adv Eng Mater **9,** 1082, 2007.
60. Detsch, R., Sarker, B., Grigore, A., and Boccaccini, A.R. Alginate and gelatine blending for bone cell printing and biofabrication. IASTED International Conference Biomedical Engineering Innsbruck. Austria: ACTA Press, 2013, pp. 451–455.

Address correspondence to:
Aldo R. Boccaccini, Dr.-Ing
Institute of Biomaterials
University of Erlangen-Nuremberg
91058 Erlangen
Germany

E-mail: aldo.boccaccini@ww.uni-erlangen.de

Rainer Detsch, Dr.-Ing
Institute of Biomaterials
University of Erlangen-Nuremberg
91058 Erlangen
Germany

E-mail: rainer.detsch@ww.uni-erlangen.de

Received: July 7, 2013
Accepted: March 19, 2014
Online Publication Date: May 9, 2014